Proyecciones Journal of Mathematics
Vol. 40, N° 6, pp. 1657-1682, December 2021.
Universidad Católica del Norte
Antofagasta - Chile

10.22199/issn.0717-6279-4357-3841

The paradox of heat conduction, influence of variable viscosity, and thermal conductivity on magnetized dissipative Casson fluid with stratification models

M. T. Akolade
A. S. Idowu
B. O. Falodun
J. U. Abubakar
University of Ilorin, Nigeria
Received : November 2019. Accepted : October 2021

Abstract

The boundary layer flow of temperature-dependent variable thermal conductivity and dynamic viscosity on flow, heat, and mass transfer of magnetized and dissipative Casson fluid over a slenderized stretching sheet has been studied. The model explores the Cattaneo-Christov heat flux paradox instead of the Fourier's law plus the stratifications impact. The variable temperature-dependent plastic dynamic viscosity and thermal conductivity were assumed to vary as a linear function of temperature. The governing systems of equations in PDEs were transformed into non-linear ordinary differential equations using the suitable similarity transformations, hence the approximate solutions were obtained using Chebyshev Spectral Collocation Method (CSCM). Effects of pertinent flow parameters on concentration, temperature, and velocity profiles are presented graphically and tabled, therein, thermal relaxation and wall thickness parameters slow down the distribution of the flowing fluid. A rise in Casson parameter, temperature-dependent thermal conductivity, and velocity power index parameter increases the skin friction thus leading to a decrease in energy and mass gradient at the wall, also, temperature gradient attain maximum within 0.2 - 1.0 variation of Casson parameter.

Keywords: *Casson fluid, Cattaneo-Christov, MHD, Spectral Collocation Method, Stratifications.*

1. Introduction

Alloy's systems such as plasma, electrolytes, and liquid metals exhibit higher thermal conductivity as a result of their effectiveness in higher possession of electrical conductivity, and transformation of energy from the heat source to the liquid. This is found applicable in power generation, MHD pumps, engineering, chemical industries among others [1]. Understanding the analysis of an electrically conducting fluid, known as Magneto fluid dynamics (MHD), basically, the concept that generates its magnetic field from the induced electric current due to the migration of the conducting fluid into a magnetic field [2]. Due to industrial and engineering applications of MHD, the attention of various researchers was drawn into the modeling of MHD in different physical characteristics, among which Mahanthesh et al. [3] presented their study on Cu-H2O nanofluid, [4] on Carbon nanotube, [5] on Carreau fluid, [2] on Water's B viscoelastic fluid, [6], [7] and [8] on Casson fluid. More recently, Kumar and Srinivas [9] highlighted that the MHD effect enhances the temperature and depreciates the velocity owing to the retarding forces opposing the flow direction.

Dated back to Crane [10] investigation of flow past a flat stretching sheet, who provided an exact solution to the quiescent fluid flow on a stretching surface, this unfolds different investigations on the flow past a stretching surface, due to its enormous applications in engineering processes and industries (glass blowing, cooling of papers, textile industry, etc.) [11]. Rao et al. [12] experiment with the slip conditions with heat transfer effect over a stretching surface. Similar studies include, results on Casson fluid are Refs. [13], [14], [15], MHD flow with a power-law velocity [16], Maxwell fluid with porous medium [17], and Nanofluid containing motile gyrotactic micro-organisms [11]. Ajayi et al. [18] presented double stratification and viscous dissipation effect on MHD Casson fluid flow over a surface with variable thickness. While recent work of Hussanan [19] considered the nonlinearly stretching sheet, Newtonian heating, and heat transfer on MHD Casson fluid flow. [20] gave the mathematical model of an isothermal sphere in MHD Casson nanofluid flow. They found a rise in Casson parameter appreciate thermal boundary layer and decline the momentum boundary layer thickness.

The importance of stratifications in geophysical flows cannot be overlooked, since it minimizes the temperature and concentration field of dissolved oxygen ([21], [22] and [23]), by negating the ambient heating from gaining access into the fluid region. Meanwhile, [24] deduced that rise in stratification

results in a reduction of velocity, velocity gradient, temperature, and temperature gradient of the fluid. However, in assuming the physical nature of problems, it is paramount to account for the thermophysical properties of such problems. Makinde et al. [25] observed that for a temperature-dependent viscosity, skin friction decreases while Nusselt number is appreciated. Animasaun et al. [14] examine that Casson fluid slows down the temperature distribution of a variable plastic dynamic viscosity, but consequently, gives rise to the velocity profile. Bearing in mind that the role of viscosity during the dissipation process cannot be neglected. Viscosity is the measure of the internal fluid friction that causes resistance to flow which is due to cohesion and interaction between the fluid particles. Dada and Adefolaju [26] reported a rise in the velocity of the fluid due to an increase in dissipation function. However, Zaib et al. [27] concluded that heat absorption at the surface is enhanced by the viscous dissipation effect.

Marin [28] asserted that Fourier's law of heat conduction is logically absurd. Since distinct material property exhibits different times necessary for the transfer of heat from one point to another (thermal relaxation time). To address this Paradox of Heat Conduction (PHC), several models of Fourier's law have been proposed of which the Maxwell-Cattenaeo model was found suitable [29]. Maxwell-Cattenaeo law was modified by Christov [29] resulting in a single system of equation for the temperature field by eliminating the heat flux. The so-called modification is thus useful for the convective heat transfer analysis. As a result, Refs. [30], [31], [32], [33], [34], [35], [36], investigated the effect of MHD flow of Casson fluid by considering the modified model, and they obtained that rise in thermal relaxation enhanced the heat transfer rate. Recently, Prasard [37] considered the theory of the Cattaneo-Christov model on Williamson Nanofluid with variable thickness. Meanwhile, the theory decelerates both concentration and temperature profiles. Nandeppanavar and Shakunthala [38], observed the impact of this model on carbon nanofluid by considering MHD along with heat transfer effects on a stretching sheet. While Zhah et al. [39] assumed an effective thermal conductivity model using the Cattaneo-Christov heat flux model in micropolar Casson ferrofluid.

Chebyshev Spectral Collocation Method (CSCM) have found satisfactorily good, excellent, and efficient in obtaining an approximate solution of both linear and non-linear, coupled and non-coupled differential equations due to its ability to handle varieties of boundary value problems ([40], [41], [22], [43]). Hence, CSCM is accorded and recommended as a powerful tool in handling both ODEs and PDEs systems [44]. Recently, [45] employed

it to solve the unsteady two-dimensional NSE. Elbarbary [46] utilized a new spectral differentiation matrix to minimize round-off error. Recently, Babatin [47], embraces this method in the study Casson fluid and heat transfer model over an unsteady stretching surface.
The literature analysis identified the gap that the combined effects of stratification and applied magnetic field over the flow assumptions on a slenderized stretching sheet with variable thermo-physical effects are still farfetched in the literature. To the author's best knowledge, using a modified heat flux model, no study is reported yet on magnetized and dissipative Casson fluid with chemically reacting fluid and variable temperature-dependent properties.

2. Formulation of the Problem

This model assumed a Cattaneo-Christov heat flux model in a free convective, two-dimensional, steady, laminar, and incompressible viscous boundary layer flow of MHD dissipative Casson fluid over a slenderized stretching sheet. The flow model and physical coordinate system were presented in Fig. 1, base on which the following flow assumptions were made:

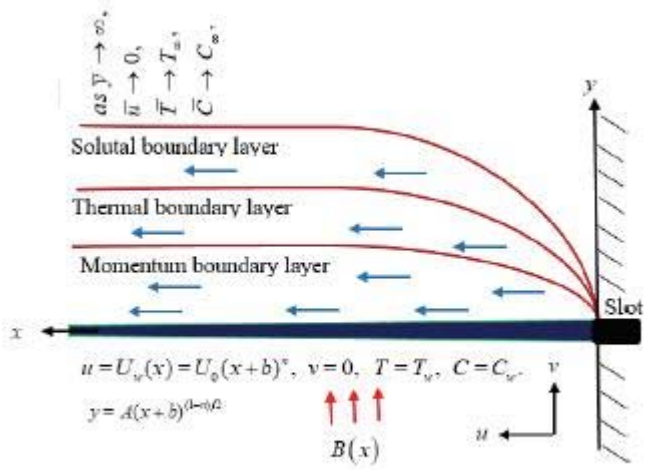

Figure 1: Flow coordinate and model analysis.

1. the flow field is assumed to be MHD conducting with magnetic field strength $B(x)$ normal to the stretching sheet in$x$ direction;
2. the sheet is assumed to be a linear function of temperature-dependent and plastic dynamic viscosity $\kappa(T) = \kappa^*[i_2 + j_2(T - T_\infty)]$ and $\mu(T) = \mu^*[i_1 + j_1(T_w - T)]$ (see Refs. [48], [49], [50], [51]), where j_2 where $j_1$are temperature-dependent thermal conductivity and plastic viscous parameter respectively;
3. Catteneo-christov heat flux model is assumed;
4. the rheology of an isotropic Casson fluid is given by $\tau_{ij} = \begin{cases} \left(\mu_b + \frac{P_y}{\sqrt{2\pi}}\right) 2e_{ij} & \text{if} \pi > \pi_c \\ \left(\mu_b + \frac{P_y}{\sqrt{2\pi_c}}\right) 2e_{ij} & \text{if} \pi < \pi_c \end{cases}$;
5. heat generation/absorption, viscous dissipation, and variations in temperature and concentration (Stratification) were assumed;
6. the velocity of the stretching sheet is $U_w = U_0(x + b)^n$, such that $n \neq 1$, hence illustrated with the profile $y = A\,(x + b)^{\frac{(1-n)}{2}} \cdot n$ denote power index, b a positive constant, U_0 the reference velocity, A is considered small corresponding to the thin of the sheet, the velocity at the free stream is assumed to be zero ($u = 0$), and the sheet is not permeable.

Considering the above assumptions along with Boussinesq approximation, the governing equation of mass, momentum, energy, and concentration is thus expressed as:

$$\frac{\partial u}{\partial x} + \frac{\partial v}{\partial y} = 0, \tag{2.1}$$

$$u\frac{\partial u}{\partial x} + v\frac{\partial u}{\partial y} = \frac{\mu_b(T)}{\rho}\left(1 + \frac{1}{\beta}\right)\frac{\partial^2 u}{\partial y^2} + \frac{1}{\rho}\left(1 + \frac{1}{\beta}\right)\frac{\partial u}{\partial y}\frac{\partial \mu_b(T)}{\partial y} - \frac{\sigma B_0^2}{\rho}u, \tag{2.2}$$

$$\begin{aligned} u\frac{\partial T}{\partial x} + v\frac{\partial T}{\partial y} \quad = \quad & \frac{k(T)}{\rho C_p}\frac{\partial^2 T}{\partial y^2} + \frac{1}{\rho C_p}\frac{\partial T}{\partial y}\frac{\partial k(T)}{\partial y}\left(1 + \frac{1}{\beta}\right) + \frac{\mu_b(T)}{\rho C_p}\left(\frac{\partial u}{\partial y}\right)^2 \pm \frac{Q_0(T - T_\infty)}{\rho C_p} + \frac{\sigma B_0^2}{\rho C_p}u^2 \\ & -h_i\left[u\frac{\partial u}{\partial x}\frac{\partial T}{\partial x} + v\frac{\partial v}{\partial y}\frac{\partial T}{\partial y} + u\frac{\partial v}{\partial x}\frac{\partial T}{\partial y} + v^2\frac{\partial^2 T}{\partial y^2} + v\frac{\partial u}{\partial y}\frac{\partial T}{\partial x} + 2uv\frac{\partial^2 T}{\partial y \partial x} + u^2\frac{\partial^2 T}{\partial x^2}\right], \end{aligned} \tag{2.3}$$

$$u\frac{\partial C}{\partial x} + v\frac{\partial C}{\partial y} = D_p\frac{\partial^2 C}{\partial y^2} - K_r(C - C_\infty), \tag{2.4}$$

boundary conditions are:

$$\begin{array}{l} u = U_w(x) = U_0(x+b)^n,\ v = 0,\ T = T_w,\ C = C_w \quad at \quad \text{y=A}(x+b)^{\frac{(1-n)}{2}} \\ u \to 0, \qquad T \to T_\infty, \qquad C \to C_\infty \qquad as \qquad y \to \infty. \end{array} \tag{2.5}$$

Were u, v are dimensionless velocity component in x and direxion $y$respectively, μ_b is the plastic dynamic viscosity, β is the Casson parameter, ρ the fluid density, B_0 represent the magnetic field strenght, σ is the fluid electrical conductivity, T is the fluid temperature, k thermal conductivity, C_p the specific heat at constant pressure, Q_0 heat generation/absorption, h_i material relaxation time C is the fluid concentration, D_p mass diffusivity, K_r chemical reaction parameter.
Following the work presented by [24], the double stratification of thermal and solutal (T_w, C_w) at the wall $(y = A\,(x+b)^{\frac{(1-n)}{2}})$ and the free stream (T_∞, C_∞) are respectively defined as:

$$\begin{array}{l} T_w - T_0 = z_1(x+b)^{\frac{1-n}{2}},\ T_\infty - T_0 = z_2(x+b)^{\frac{1-n}{2}}, \\ C_w - C_0 = z_3(x+b)^{\frac{1-n}{2}},\ C_\infty - C_0 = z_4(x+b)^{\frac{1-n}{2}}. \end{array} \tag{2.6}$$

Hence, these relations hold:

$$j_1(T_w - T_0) = j_1 z_1(x+b)^{\frac{1-n}{2}}, \quad j_1(T_\infty - T_0) = j_1 z_2(x+b)^{\frac{1-n}{2}}\ . \tag{2.7}$$

T_0 been the reference temperature, there exist two differences in temperature: first due to stratification which occurs for all x at a fixed point of $y = A(x+b)^{\frac{1-n}{2}}$ and the latter occurs for all x as $y \to \infty$. Hence, temperature-dependent thermal conductivity γ, and the plastic dynamic viscosity $\delta$are defined as: $\gamma = j_2(T_\infty - T_0)$ and $\delta = j_1(T_\infty - T_0)$ respectively, along with the relation $\gamma\varphi = j_2(T_w - T_0)$ and $\delta\varphi = j_1(T_w - T_0)$. The ratio of Eq. EQ7 thus produces the dimensionless stratification parameters, thermal and solutal $\varphi = \frac{T_w - T_0}{T_\infty - T_0} = \frac{z_1}{z_2}$ and $\varrho = \frac{C_w - C_0}{C_\infty - C_0} = \frac{z_3}{z_4}$ respectively.
Transforming the governing PDEs in Eqns. EQ1-EQ4 together with $EQ5$ into an ODEs, using similarity transformations below as utilized in ([7], [8]).

$$\begin{array}{l} u=\frac{\partial\psi}{\partial y}, \quad v=-\frac{\partial\psi}{\partial x} \quad \psi=\left(\frac{2\nu U_{\circ}(x+b)^{n+1}}{n+1}\right)^{\frac{1}{2}} f(\eta), \\ \eta=\left(\frac{(n+1)U_{\circ}(x+b)^{n-1}}{2v}\right)^{\frac{1}{2}} y, \;\; \theta(\eta)=\frac{T-T_{\infty}}{T_w-T_{\infty}}, \quad \phi(\eta)=\frac{C-C_{\infty}}{C_w-C_{\infty}}. \end{array} \tag{2.8}$$

Where ψ is the stream function, ν represent the kinematic viscosity, $f(\eta)$ is the dimensionless velocity, $\theta(\eta)$ is the dimensionless temperature, ϕ is the dimensionless concentration, and η is the dimensionless distance. Utilizing the stream function $u=\frac{\partial\psi}{\partial y}$, $v=-\frac{\partial\psi}{\partial x}$ given in Eq. EQ8, then equation EQ1 is automatically satisfied, also invoking EQ8 in Eqs. EQ2-EQ5 we have;

$$\left(1+\frac{1}{\beta}\right)\left[Q_1 f'''(\eta)-\delta\theta'(\eta)f''(\eta)\right]+f(\eta)f''(\eta)-\left(\frac{2}{n+1}\right)\left[n\left(f'(\eta)\right)^2+M^2 f'(\eta)\right]=0 \tag{2.9}$$

$$\begin{array}{c} Q_2\theta''(\eta)+\gamma\left(\theta'(\eta)\right)^2-P_r\left(\frac{1-n}{n+1}\right)\theta(\eta)f'(\eta)-P_r\varphi\left(\frac{1-n}{n+1}\right)f'(\eta)+E_c\,\mathrm{Pr}\,HaM^2\left(f'(\eta)\right)^2, \\ -P_r h_o\left[\left(\frac{n+1}{2}\right)f(\eta)\theta'(\eta)f'(\eta)-\left(\frac{(n-1)^2}{2(n+1)}\right)\left(f(\eta)\right)^2\theta(\eta)-\varphi\left(\frac{(n-1)^2}{2(n+1)}\right)\left(f'(\eta)\right)^2+\right. \\ \left.\left(\frac{n-1}{2}\right)f(\eta)\theta(\eta)f''(\eta)+\varphi\left(\frac{n-1}{2}\right)f(\eta)f''(\eta)+\left(\frac{n+1}{2}\right)f^2(\eta)\theta''(\eta)\right]+P_r\theta'(\eta)f(\eta) \\ +E_cP_rQ_1\left(1+\frac{1}{\beta}\right)\left(f''(\eta)\right)^2+P_rH_0\left(\frac{2}{n+1}\right)\theta(\eta)=0, \end{array} \tag{2.10}$$

$$\phi''(\eta)+S_c f(\eta)\phi'(\eta)+\left(\frac{n-1}{n+1}\right)\left[S_c f'(\eta)\phi(\eta)+S_c\varrho f'(\eta)\right]-S_c\lambda\left(\frac{2}{n+1}\right)\phi(\eta)=0, \tag{2.11}$$

For simplicity, we let $Q_1=[i_1+\delta-\delta\theta(\eta)-\delta\varphi]$ and $Q_2=[i_2+\gamma\theta(\eta)]$. Since the sheet is stretching, hence, $\eta=A\left(\frac{(n+1)U_0}{2\nu}\right)^{\frac{1}{2}}$ is assumed as the least similarity variable. Then, the boundary condition becomes;

$$\begin{array}{l} f(\chi)=\chi\left(\frac{1-n}{1+n}\right), \quad f'(\chi)= \quad \theta(\chi)= \quad \phi(\chi)=1 \quad \text{for} \quad \eta=\chi, \\ f'(\infty)\to 0, \qquad \theta(\infty)\to 0, \qquad \phi(\infty)\to 0 \qquad \text{for} \quad \eta\to 0. \end{array} \tag{2.12}$$

where $\chi = A\left(\frac{(n+1)U_0}{2\nu}\right)^{\frac{1}{2}}$ represent the plate surface. Equations $EQ9$ - $EQ11$ along with $EQ12$ are in the domain $[\chi, \infty)$. Dimensionalizing into $[0, \infty)$ we set $g(\tau) = g(\eta - \chi) = f(\eta)$, $h(\tau) = h(\eta - \chi) = \theta(\eta)$ and $\Phi(\tau) = \Phi(\eta - \chi) = \phi(\eta)$ then we have:

$$\left(1 + \frac{1}{\beta}\right)\left[Q_3 g'''(\tau) - \delta h'(\tau) g''(\tau)\right] + g(\tau) g''(\tau) - \left(\frac{2}{n+1}\right)\left[n\left(g'(\tau)\right)^2 + M^2 g'(\tau)\right] = 0, \tag{2.13}$$

$$\begin{aligned} &Q_4 h''(\tau) + \gamma\left(h'(\tau)\right)^2 - P_r\left(\tfrac{1-n}{n+1}\right) h(\tau) g'(\tau) - P_r\varphi\left(\tfrac{1-n}{n+1}\right) g'(\tau) + E_c \Pr HaM^2 \left(g'(\tau)\right)^2 - \\ &P_r h_o\left[\left(\tfrac{n+1}{2}\right) g(\tau) h'(\tau) g'(\tau) - \left(\tfrac{(n-1)^2}{2(n+1)}\right)\left(g(\tau)\right)^2 h(\tau) - \varphi\left(\tfrac{(n-1)^2}{2(n+1)}\right)\left(g'(\tau)\right)^2 + \right. \\ &\left.\left(\tfrac{n-1}{2}\right) g(\tau) h(\tau) g''(\tau) + \varphi\left(\tfrac{n-1}{2}\right) g(\tau) g''(\tau) + \left(\tfrac{n+1}{2}\right) g^2(\tau) h''(\tau) + P_r h'(\tau) g(\tau)\right] + \\ &E_c P_r Q_3\left(1 + \tfrac{1}{\beta}\right)\left(g''(\tau)\right)^2 + P_r H_0\left(\tfrac{2}{n+1}\right) h(\tau) = 0, \end{aligned} \tag{2.14}$$

$$\Phi''(\tau) + S_c g(\tau)\Phi'(\tau) + \left(\frac{n-1}{n+1}\right)\left[S_c g'(\tau)\Phi(\tau) + S_c \varrho g'(\tau)\right] - S_c\lambda\left(\frac{2}{n+1}\right)\Phi(\tau) = 0, \tag{2.15}$$

and the boundary conditions give;

$$\begin{aligned} &g(0) = \chi^{\frac{(1-n)}{1+n}}, \qquad g'(0) = h(0) = \Phi(0) = 1, \\ &g'(\infty) \to 0, \qquad h(\infty) \to 0, \qquad \Phi(\infty) \to 0. \end{aligned} \tag{2.16}$$

Where $Q_3 = [i_1 + \delta - \delta h(\tau) - \delta\varphi]$ and $Q_4 = [i_2 + \gamma h(\tau)]$, $M = \frac{\sigma B_0^2}{\rho U_o}$, $P_r = \frac{C_p \mu}{k^*}$, $h_o = h_i U_o (x+b)^{n-1}$, $\delta = j_1\left(T_\infty - T_0\right)$, $\gamma = j_2\left(T_\infty - T_0\right)$, $H_0 = \frac{Q_0}{\rho C_p}$, $S_c = \frac{\nu}{D_p}$, $\lambda = \frac{K_r}{\rho C_p U_0}$, $\varphi = \frac{z_1}{z_2}$, $\varrho = \frac{z_3}{z_4}$, $\chi = A\left(\frac{(n+1)U_0}{2\nu}\right)^{\frac{1}{2}}$, $E_c = \frac{U_0^2 (x+b)^{2n}}{C_p z_2 (x+b)^{\frac{1-n}{2}}}$ and i_1, i_2 are taken to be unity.

where β, γ, φ, ϱ, H_0, δ, E_c, n, S_c, M, χ, λ, P_r, h_o are Casson parameter, temperature-dependent thermal conductivity, thermal stratification parameter, solutal stratification parameter, heat generation/absorption parameter, temperature-dependent plastic dynamic viscosity, Eckert number, velocity power index parameter, Schmidt number, magnetic field parameter, wall thickness parameter, chemical reaction parameter, Prandtl number, and thermal relaxation parameter respectively.

3. Method of Solution

The Chebyshev Spectral Collocation Method (CSCM) known for its efficiency and accuracy in handling highly nonlinear systems of equations ([41], [42],[52]) is utilized in this study. In the implementation of CSCM, we employed the domain truncation approach to approximate the problem domain $[0, \infty)$into $[0, \mathrm{L}]$. L being the scaling parameter is used to indicate the convergence at infinity (see, [41], [42], [49]). CSCM assumes an unknown trial functions $g(\tau)$, $h(\tau)$ and $\Phi(\tau)$ which are then approximated by the sum of basis function $T_k(\tau)$with the unknown constants a_k, b_k and c_k to be determined.

$$(3.1)\quad \begin{aligned} g(\tau) \approx g_N(\tau) &= \textstyle\sum_{k=0}^{N} a_k T_k(\tau),\ h(\tau) \approx h_N(\tau) = \sum_{k=0}^{N} b_k T_k(\tau), \\ &\quad \Phi(\tau) \approx \Phi_N(\tau) = \textstyle\sum_{k=0}^{N} c_k T_k(\tau), \end{aligned}$$

By substituting Eq.$EQ17$ into boundary condition EQ16, we as well substitute into the governing Eqs. $(13-15)$ then the non-zero residue is obtained. To minimize error, residues are equated to zero at N collocation points. However, minimization of the expected residue depends on the coefficient a_k, b_k, and c_k assumed. Chebyshev collocation points used are defined by [52].

$$(3.2)\qquad \tau_j = \cos\left(\frac{\pi j}{N}\right), \qquad j = 0, 1, 2, ..., N$$

Owing to this, a system of $3N + 3$ algebraic equations with $3N + 3$ unknown coefficient expansion a_k, b_k and c_k is obtained. And Newton iteration method (Finlayson [53]) is thus employed to solve the derived algebraic equations. The Mathematical symbolic package used is MATHEMATICA. The obtained values of constants a_k, b_k, and c_k are substituted into equation Eq. EQ17 to get the required approximate result.

4. Numerical Computations and Discussion of Results

In this section, we considered the pertinent parameters as $n = H_0 = \lambda = h_0 = \varrho = \varphi = \chi = 0.1$ $P_r = 0.72$, $E_c = \delta = \gamma = 0.5$, $\beta = 0.2$, $M = 1$, $Sc = 0.62$. These values are kept constant throughout the experiment else stated otherwise.
To authenticate the method used in this study, new terms added were set to zero and the following corresponding results were obtained by Chebyshev Spectral Collocation Method (CSCM). Table 1 compared the present result with that of Nadeem *et al.* [54] where ADM along with Pade approximation was used. And different values of Prandtl number as stated in Pramanik [55]. Table 2 compared the result of skin friction and heat transfer coefficient with that of Ref. [7] who adopted the shooting method along with classical Runge-Kutta.

Table 4.1: Comparison of the Skin friction coefficient $[g''(0)]$ (Nadeem et al. [51]) and heat transfer coefficient $[-h'(0)]$ (Pramanik [52]). Where $\Gamma = \left(1 + \frac{1}{\beta}\right)$

For $n = 2$, $\beta = 1$ and varying χ & M				For $n = 1$, $\beta \to \infty$ varying Pr		
χ	M	Present study $\Gamma g''(0)$	Nadeem *et al.* [47] $\Gamma g''(0)$	Pr	Present study $-h'(0)$	Pramanik [48] $-h'(0)$
-3	2^2	1.366679	1.36668	1	0.955216	0.9547
-3	3^2	2.184183	2.184183	2	1.471361	1.4714
$-\frac{3}{2}$	2^2	1.215503	1.215503	3	1.868998	1.8691
				5	2.500074	2.5001
				10	3.660627	3.6603

Table 4.2: Comparison, Skin friction coefficient $[g''(0)]$ and heat transfer coefficient $[-h'(0)]$ for different values of n and χ when $Pr = 0.7$, $\beta \to \infty$ and $Ec = \delta = \gamma = Sc = H_0 = \lambda = h_0 = \varrho = \varphi = 0$.

		Present study		Nadeem et al. [51]	
n	χ	$[g''(0)]$	$[-h'(0)]$	$[g''(0)]$	$[-h'(0)]$
-0.5	0.5	-1.16666855	1.90452127	-1.16668224	1.90459332
-0.5	0.25	-0.08338680	1.73607330	-0.08365155	1.73611251
$-\frac{1}{3}$	0.25	-0.50009300	1.34269600	-0.50041742	1.34290940

Table 4.1 displays the numerical computations depicting the effect of parameters on the flow, bearing in mind that other pertinent parameters remain the same as stated earlier in this section. It was observed that a rise in parameter β, n, and γ increases the Skin friction and leads to a decrease in the energy and mass gradient at the wall. But β tend to attain the maximum value of temperature gradient within the range of $0.2 - 1.0$ and declined afterward. Meanwhile, the addition M, h_0 and δ eventually decreases the Sherwood number Skin friction and Nusselt number. Also, increase χ and Pr reduces skin friction and thus accelerates the temperature and concentration gradient.

Table 3: Computed effects of β, M, δ, γ, n, h_0, Pr and χ on Skin friction $[\Gamma g''(0)]$, heat transfer $-h'(0)$ and mass transfer coefficients $-\Phi'(0)$. where $\Gamma = \left(1 + \frac{1}{\beta}\right)$

Values		$[\Gamma g''(0)]$	$-h'(0)$	$-\Phi'(0)$	Values		$[\Gamma g''(0)]$	$-h'(0)$	$-\Phi'(0)$
β	0.1	-5.59247486	0.1770193178	0.957091728	h_0	0	-4.06291010	0.2302894562	0.918161778
	0.5	-2.835951590	0.233680834	0.858556713		0.1	-4.06665031	0.2301594690	0.918120515
	1	-2.299385061	0.2065882874	0.816728263		0.3	-4.07437670	0.230036910	0.91803718
	1.5	-2.093466865	0.1874745755	0.796565990		0.5	-4.08223560	0.229846146	0.917954250
M	0	-2.159398840	0.5189922000	0.992106653	n	0.1	-4.06665032	0.2301594689	0.918120515
	1	-4.06665032	0.2301594689	0.918120515		0.3	-3.945226384	0.1566960229	0.806440287
	2	-5.28096019	0.01342416390	0.870878306		0.5	-3.853767675	0.0973804777	0.717744511
	3	-6.22960757	-0.1632299379	0.835962125		0.7	-3.782215666	0.0480339083	0.645157108
δ	0	-3.7454662	0.2639588253	0.923280391	γ	0	-4.10156775	0.279676751	0.918589690
	1	-4.39056771	0.1980186777	0.91226014		0.5	-4.06665031	0.2301594689	0.918120515
	2	-5.06014418	0.1383759489	0.898627054		1	-4.03991428	0.1986482341	0.917935200
	3	-5.78079501	0.0856307559	0.882334776		1.5	-4.01847970	0.1757166117	0.917886024
χ	0.1	-4.06665032	0.2301594689	0.918120515	Pr	0.5	-4.03034794	0.1976834674	0.918116368
	0.3	-4.17792814	0.2684542540	0.979868056		0.7	-4.063781109	0.2277012294	0.918116097
	0.5	-4.290386850	0.309263052	1.044307037		1	-4.09944173	0.2558173921	0.918228520
	0.7	-4.40397472	0.35257511	1.111261349		2	-4.15966601	0.2773167879	0.918746799

The figure 2 represents the behavior of $h_0$the on energy profile, and it was found to decrease in temperature field as thermal relaxation parameter increases, i.e. material particle needed extra time for heat transfer to its surrounding particle due to thermal relaxation enhancement in temperature of the Casson fluid. Physically, thermal diffusion with an increasing function of Prandtl number decreases which amounts to boundary layer thickness, hence, a decrease in temperature field is seen perceived in Fig.3.

The figure 7 displays the variations in velocity profile for the various value of the Magnetic parameter (M). Increasing M results in a decrease of the profile $g'(\tau)$, this amount to the transverse magnetic field creating a Lorentz force corresponding to drag force which act as a retarding force, and hence provide resistance to the momentum boundary layer. Consequently, the rise in (M) produce a significant temperature rise field as displayed in Fig. 8. The figure $9-11$ presents the effects of βon energy and mass transfer respectively.

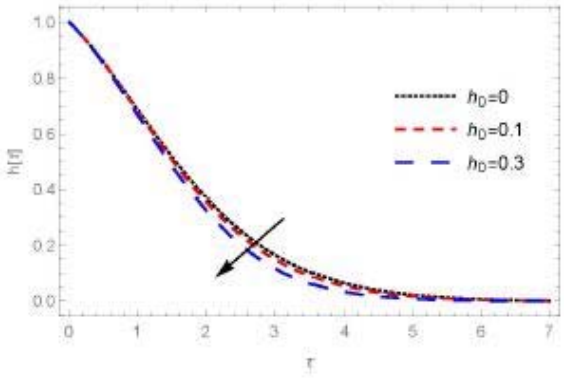

Figure 2: Effect of h_0 on temperature profile.

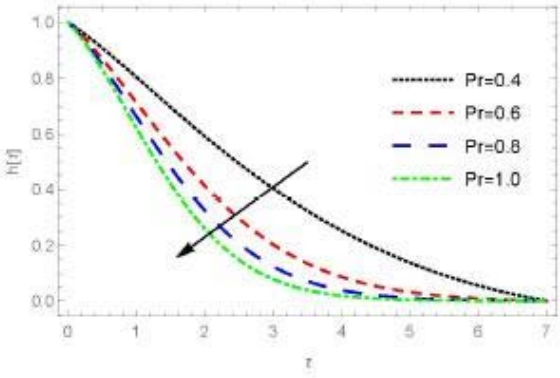

Figure 3: Effect of Pr on temperature profile.

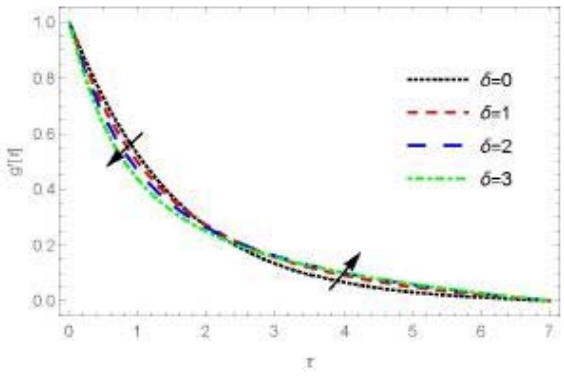

Figure 4: Effect of δ on velocity profile.

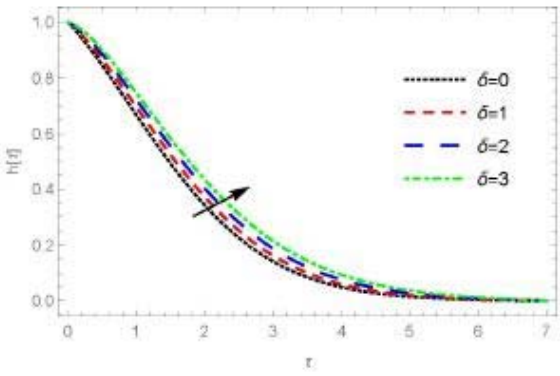

Figure 5: Effect of δ on temperature profile.

The effect of temperature-dependent plastic dynamic viscosity (δ) on the flow and energy transfer are presented in Fig. 4 and 5. Rise in pertinent values δ reduces the fluid velocity near the stretching surface at $\tau \leq 2$ but it increases as it moves away from the surface, while an increase in δ enhancing the energy field, the thermal boundary layer, however, reduces heat transfer while it gives no significant effect on the concentration profile. The figure 6 presents an increment in the energy profile of the Casson fluid and reduces it into the free stream region with an increasing value of temperature-dependent thermal conductivity parameter (γ), this affects the boundary layer to generate heat and assist temperature profiles. Meanwhile, (γ) shows no significant effect on flow and mass transfer profiles.

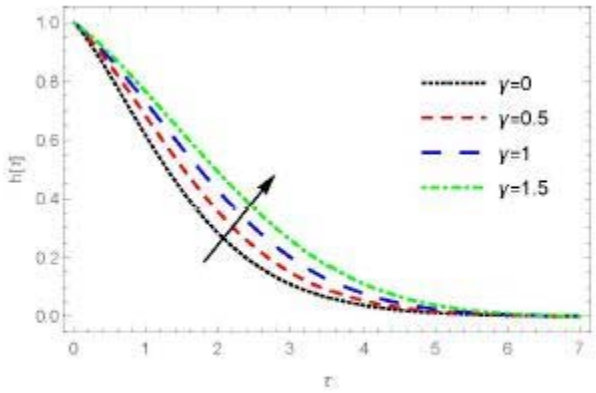

Figure 6: Effect of γ on temperature profile.

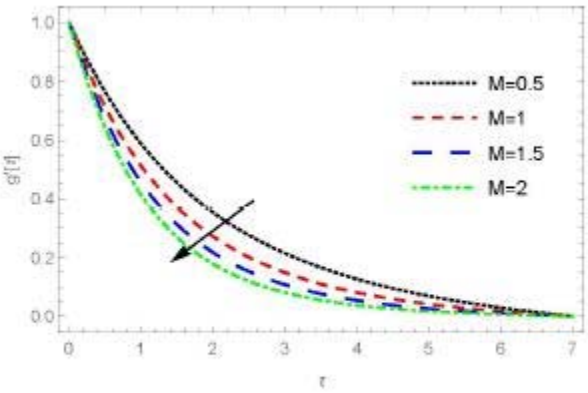

Figure 7: Effect of M on velocity profile.

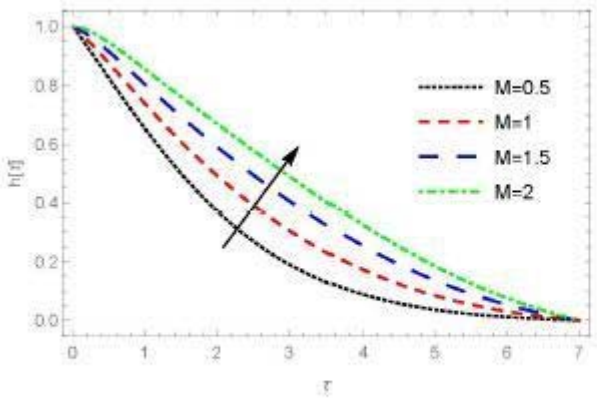

Figure 8: Effect of M on temperature profile.

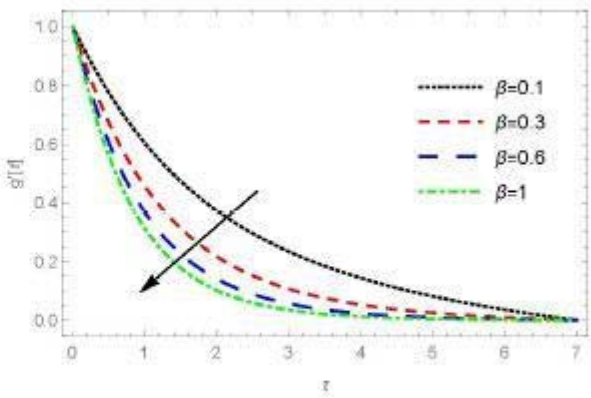

Figure 9: Effect of β on velocity profile.

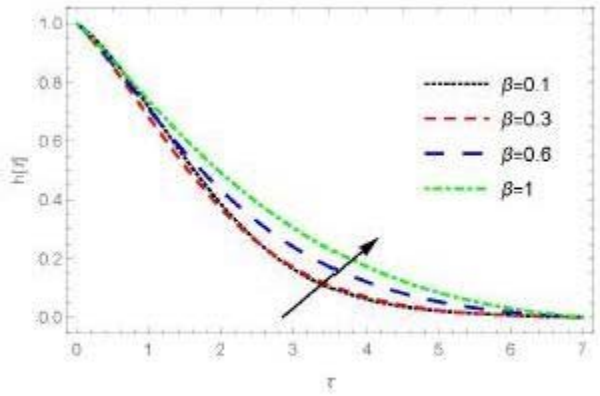

Figure 10: Effect of β on temperature profile.

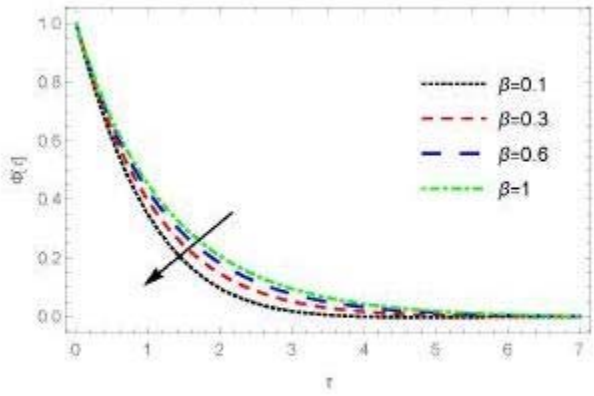

Figure 11: Effect of β on Velocity profile.

The figure 7 displays the variations in velocity profile for the various value of the Magnetic parameter (M). Increasing M results in a decrease of the profile $g'(\tau)$, this amount to the transverse magnetic field creating a Lorentz force corresponding to drag force which act as a retarding force, and hence provide resistance to the momentum boundary layer. Consequently, the rise in (M) produce a significant temperature rise field as displayed in Fig. 8. The figure $9-11$ presents the effects of βon energy and mass transfer respectively.

In Fig. 9, the velocity field decreases with a rise in βparameter, while in Fig. 10 β gives rise to the temperature profile across the flow field. Practically, increasing β gives rise to the plastic dynamic viscosity, meaning an increase in β reduced yield stress of Casson fluid (resistivity force), contrary to the result obtained in Fig. 10, this is viewed as a result of a decrease in fluid temperature which is overpowered by the high amount of temperature injected. And a decrease in the mass transfer of Casson fluid is observed as we increase β as depicted in Figure 11.

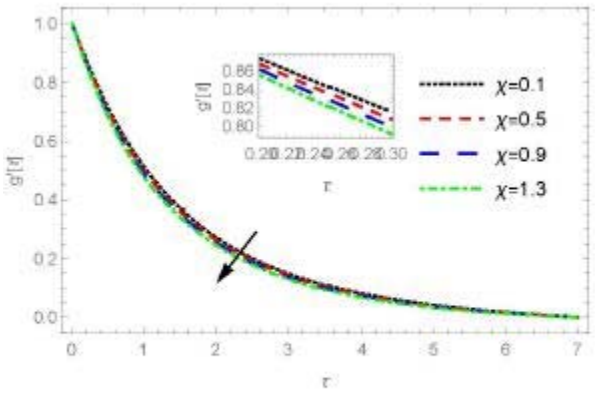

Figure 12: Effect of χ on velocity profile.

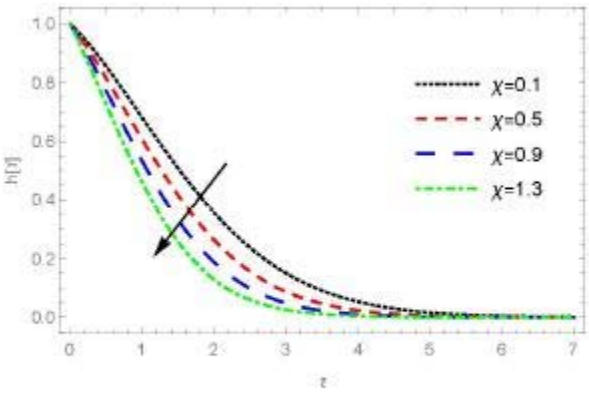

Figure 13: Effect of χ on temperature profile.

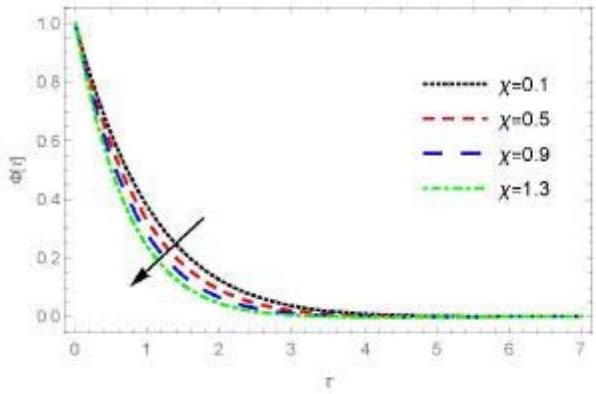

Figure 14: Effect of χ on concentration profile.

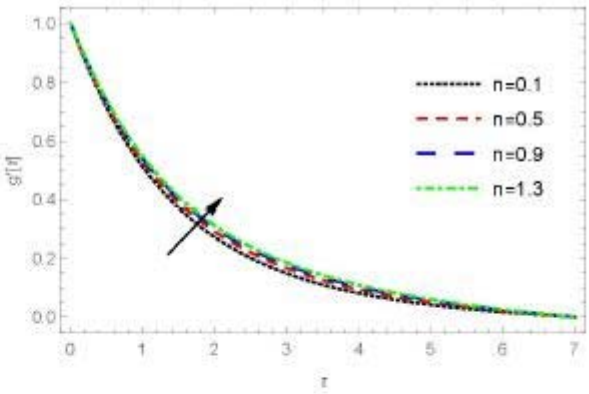

Figure 15: Effect of n on velocity profile.

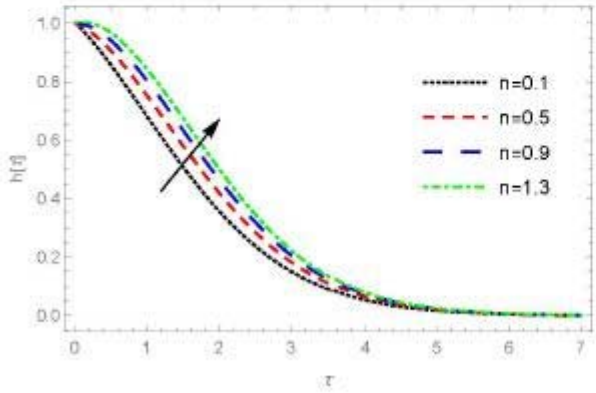

Figure 16: Effect of n on temperature profile.

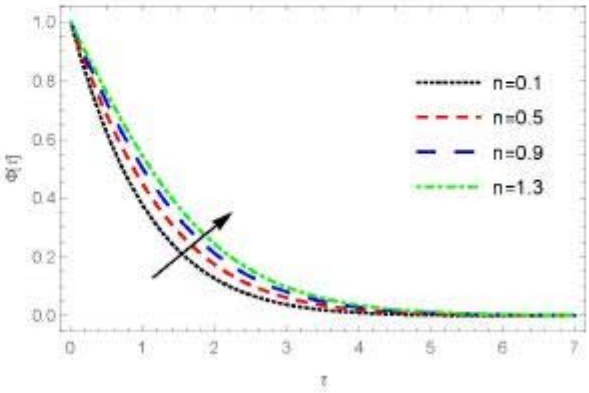

Figure 17: Effect of n on concentration profile.

Ec gave rise to the temperature profile due to heat energy stored in the liquid because of frictional heating. While a rise in Ec decreases the velocity distribution as pictured in Fig. 19. Figure 20 indicates the behavior of heat generation/absorption parameter H_0 on temperature distribution. In both cases of heat generation ($H_0 > 0$) and absorption ($H_0 < 0$) more heat is produced which results in the enhancement of the temperature field. The figure 21 displayed that the larger value of the chemical reaction parameter (λ) decelerates the fluid concentration along with boundary layer thickness. Moreover, the concentration of the fluid is observed to reduce significantly with an increasing value of Sc as presented in Fig. 22. Thermal stratification (φ) give a declined behavior towards the temperature field owing to the reduction in effective temperature difference, as shown in Fig. 23. Similarly Fig. 24 presents the reduction in the concentration of the Casson fluid as Solutal stratification increases.

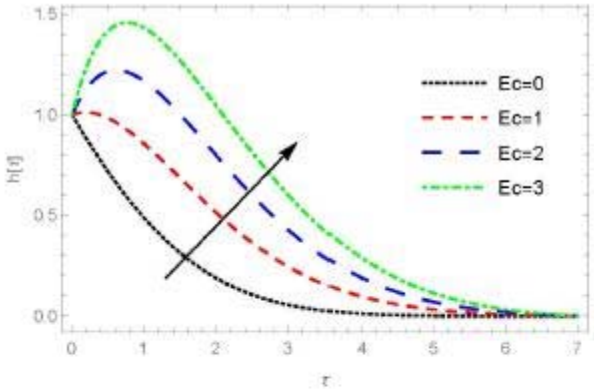

Figure 18: Effect of Ec on temperature profile.

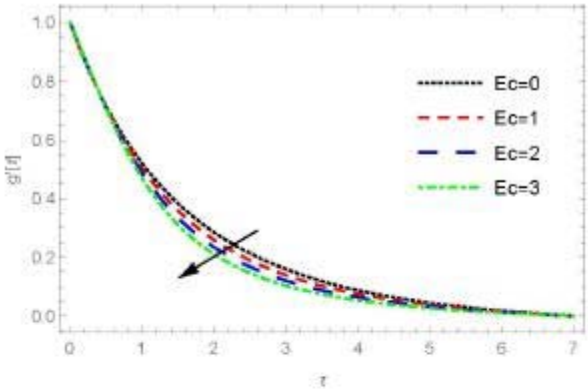

Figure 19: Effect of Ec on velocity profile.

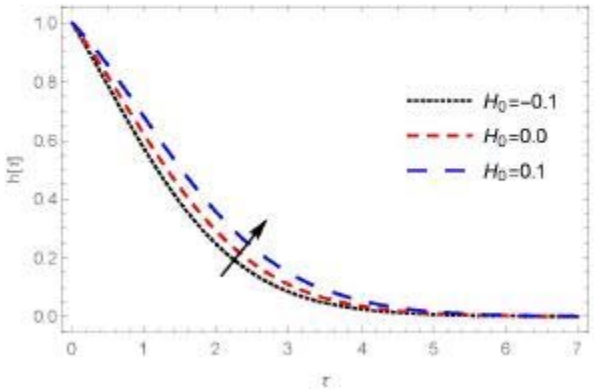

Figure 20: Effect of H_0 on temperature profile.

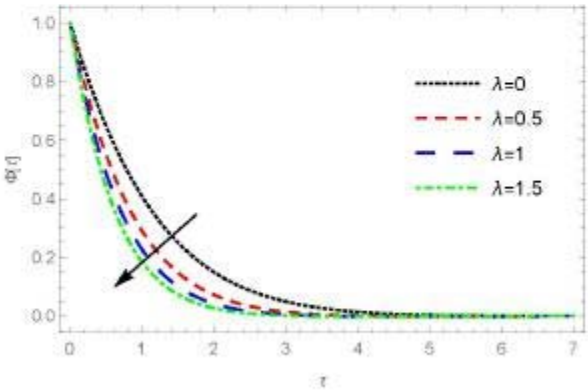

Figure 21: Effect of λ on concentration profile.

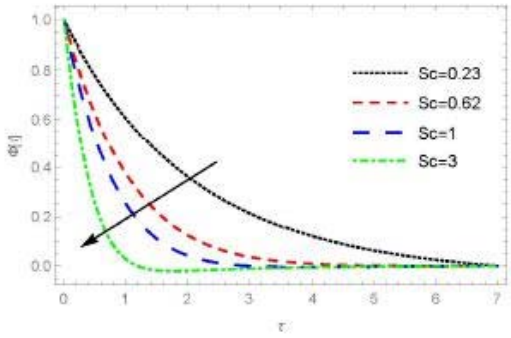

Figure 22: Effect of Sc on concentration profile.

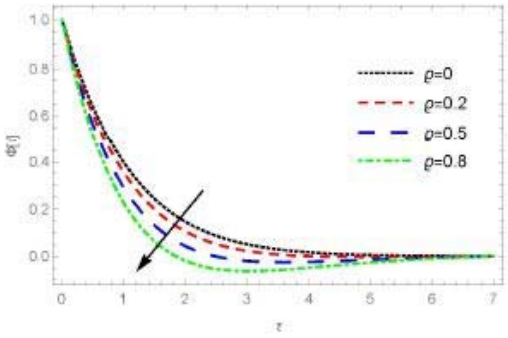

Figure 23: Effect of ϱ on concentration profile.

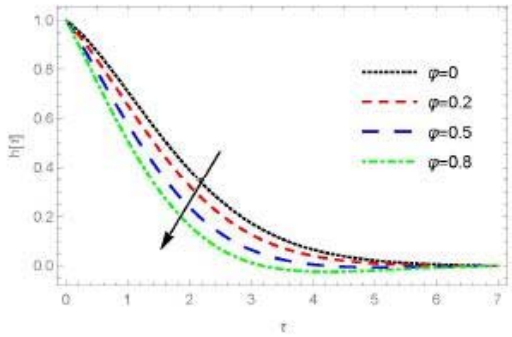

Figure 24: 24. Effect of φ on temperature profile.

5. Conclusion

A study on boundary layer flow of dissipative and magnetized Casson fluid was formulated by incorporating the paradox of heat conduction, variable viscosity, thermal conductivity, and stratification influence over a slenderized stretching sheet. The governing nonlinear coupled ordinary differential equations responsible for the flow model were solved using Chebyshev Spectral Collocation Method (CSCM). From these investigations, the findings based on the study were as follows:

1. existence of thermal relaxation time brings down the temperature distribution.

2. the introduction of the magnetic field effect reduces the velocity field across the boundary layer and appreciates in the temperature profile.

3. increase in Prandtl's number reduces the velocity profile.

4. reduction in velocity and concentration profiles were noticed by higher Casson parameters while appreciating the temperature profile.

5. temperature-dependent plastic dynamic viscosity gives rise to rising velocity and temperature profiles, but it initially decreases the velocity and increases as it goes into the free stream. Moreover, temperature-dependent thermal conductivity appreciates the temperature profile.

6. introduction of wall thickness parameter brings down the fluid flow, energy, and mass transfer of the Casson fluid, while these profiles were appreciated in the variations of the velocity power index.

7. rise Schmidt's number, chemical reaction, and solutal stratification reduce the fluid concentration.

8. heat generation/absorption increases the velocity while thermal thermal stratification declined the temperature field.

9. Eckert number increases the temperature decreases the velocity and towards the wall but decreases along the free stream.

References

[1] A. Miner and U. Ghoshal, "Cooling of high-power-density microdevices using liquid metals coolants", *Applied physics letters*, vol. 85, no. 3, pp. 506-508, 2004.

[2] A. S. Idowu and B. O. Falodun, "Soret-Dufour e ects on MHD heat and mass transfer of Walter's-B viscoelastic fluid over a semi-infinite vertical plate: spectral relaxation analysis", *Journal of Taibah University for Science*, vol. 13, no. 1, pp. 49-62, 2019.

[3] B. Mahanthesh, B. J. Gireesha, and R. S. R. Gorlac, "Heat and mass transfer e ects on the mixed convective flow of chemically reacting nanofluid past a moving/stationary vertical plate", Alexandria engineering journal, vol. 55, no. 1, pp. 569-581, 2016.

[4] S. Nasir, Z. Shah, S. Islam, W. Khan, and S. N. Khan, "Radiative flow of magneto hydrodynamics single-walled carbon nanotube over a convectively heated stretchable rotating disk with velocity slip e ect", *Advances in mechanical engineering*, vol. 11, no. 3, pp. 1-11, 2019.

[5] S. Bilal, Shafqatullah, A. S. Alshomrani, M. Y. Malik, N. Kausar, F. Khan, and K. Rehman, "Analysis of Carreau fluid in the presence of thermal stratification and magnetic field e ect", *Result in physics*, vol. 10, pp. 118-125, 2018.

[6] E. M. Arthur,I. Y. Seini, and L. B. Bortteir, "Analysis of Casson fluid flow over a vertical porous surface with chemical reaction in the presence of magnetic field", *Journal of applied mathematics and physics*, vol. 3, pp. 713-723, 2015.

[7] T, M. Ajayi, A. J. Omowaye and I. L. Animasaun," E ects of viscous dis sipation and double stratification on MHD Casson fluid flow over a surface with variable thickness: boundary layer analysis", *International journal of engineering research in Africa*, vol. 28, pp. 73-89, 2017.

[8] M. Y. Malik, M. Khan, T. Salahuddin, and I. Khan, I., "Variable viscosity and MHD flow in Casson fluid with Cattaneo-Christov heat flux model: Using Keller box method", *Engineering science and technology an international journal*, vol. 19, pp. 1985-1992, 2016.

[9] B. Kumar and S. Srinivas, "Unsteady hydromagnetic flow of Eyring-Powell nanofluid over an inclined permeable stretching sheet with joule heating and thermal radiation", *Journal of applied and computational mechanics*, vol. 6, no., 2, pp. 259-270, 2020.

[10] L. J. Crane, "Flow past a stretching plate", *Zeitschrift für angewandte mathematik und physik*, vol. 21, 1970, pp. 645-647, 1970.

[11] S. A. M. Mehryan, F. M. Kashkooli, M. Soltani, and K. Raahemifar, "Fluid flow and heat transfer analysis of a nanofluid containing motile gyrotactic micro-organisms passing a nonlinear stretching vertical sheet in the presence of a non-uniform magnetic field; numerical approach", *PLoS ONE*, vol. 11, no. 1, 2016.

[12] A. S. Rao, V., Prasad, N. Nagendra, K., Murthy, N. Reddy, and O. Beg, "Numerical modeling of non-similar mixed convection heat transfer over a stretching surface with slip conditions", *World journal of mechanics*, vol. 5, no. 6, pp. 117-128, 2015.

[13] T. C. Chiam, "Hydromagnetic flow over a surface stretching with a power-law velocity", *International journal of engineering science*, vol. 33, no. 3, pp. 429-435, 1995.

[14] I. L. Animasaun, E. A. Adebile, and A. I. Fagbade, "Casson fluid flow with variable thermo-physical property along exponentially stretching sheet with suction and exponentially decaying internal heat generation using the homotopic analysis method", *Journal of the Nigerian Mathematical Society*, vol. 35, no. 1, pp. 1-17, 2016.

[15] N. A. Khan and S. Khan, "Dual solution of Casson fluid over a porous medium: Exact solutions with extra boundary condition", *ACTA Universitatis Cibiniensis*, vol. 68, no. 1, pp. 35-49, 2016.

[16] M. Y. Malik, M. Khan, T. Salahuddin, and I. Khan, "Variable viscosity and MHD flow in Casson fluid with Cattaneo-Christov heat flux model: Using Keller box method", *Engineering science and technology an international journal*, vol. 19, pp. 1985-1992, 2016.

[17] V. Singh and S. Agarwal, "MHD flow and heat transfer for Maxwell fluid over an exponentially stretching sheet with variable thermal conductivity in porous medium", *Thermal science*, vol. 18, no. sup. 2, pp. 599-615, 2014.

[18] T. M. Ajayi, A. J. Omowaye, and I. L. Animasaun, "E ects of viscous dissipation and double stratification on MHD Casson fluid flow over a surface with variable thickness: boundary layer analysis", *International journal of engineering research in Africa*, vol. 28, pp. 73-89, 2017.

[19] A. Hussanan, M. Z. Salleh, H. T. Alkasasbeh, and I. Khan, "MHD flow and heat transfer in a Casson fluid over a nonlinearly stretching sheet with newtonian heating", *Heat transfer research*, vol. 49, no. 12, pp. 1185-1198, 2018.

[20] A. S. Rao, S. Sainath, P. Rajendra, and G. Ramu, "Mathematical modelling of hydromagnetic Casson non-newtonian nanofluid convection slip flow from an isothermal sphere", *Nonlinear engineering*, vol. 8, no. 1, 2019, 645-660, 2019.

[21] E. Sebnem, "E ects of thermal stratification and mixing on reservoir water quality", *The Japanese Society of Limnology*, vol. 9, pp. 135-142, 2008.

[22] F. H. M. S. Noor, S. A. A. Ahmad, and M. A. Zaileha, "Double stratification e ects on boundary layer over a stretching cylinder with chemical reaction and heat generation", *Journal of physics: Conference series*, vol. 890, no. 1, Art. ID. 012019, 2017.

[23] W. N. Mutuku and O. D. Makinde, "Double stratification e ects on heat and mass transfer in unsteady MHD nanofluid flow over a flat surface". *Asia pacific journal computational engineering*, vol. 4, Art. ID. 2, 2017.

[24] A. J. Omowaye and I. L. Animasaun, "Upper-convected maxwell fluid flow with variable thermo-physical properties over a melting surface situated in hot environment subject to thermal stratification", *Journal of applied fluid mechanics*, vol. 9, no. 4, pp. 1777-1790, 2016.

[25] O. D. Makinde, W. A. Khan, and J. R. Culham, "MHD variable viscosity reacting flow over a convectively heated plate in a porous medium with thermophoresis and radiative heat transfer", *International journal of heat and mass transfer*, vol. 93, pp. 595-604, 2016.

[26] M. S. Dada, and F. H. Adefolaju, "Dissipation, MHD and radiation effects on an unsteady convective heat and mass transfer in a Darcy-Forcheimer porous medium", J*ournal of mathematics research*, vol. 4, no. 2, pp. 110-127, 2012.

[27] A. Zaib, K. Bhattacharyya, M. S. Uddin, and S. Shafie, "Dual solutions of non-newtonian Casson fluid flow and heat transfer over an exponentially permeable shrinking sheet with viscous dissipation", *Modelling and simulation in engineering*, vol. 2016. Art. ID. 6968371, 2016.

[28] E. Marín, "Does Fourier's law of heat conduction contradict the theory of relativity?", *Latin-american journal of physics education*, vol. 5, no. 2, pp. 402-405, 2011.

[29] C. I. Christov, "On frame indi erent formulation of the Maxwell-Cattaneo model of finite-speed heat conduction", *Mechanics research communications*, vol. 36, pp. 481-486, 2009.

[30] M. Y. Malik, M. Khan, T. Salahuddin, and I. Khan, "Variable viscosity and MHD flow in Casson fluid with Cattaneo-Christov heat flux model: Using Keller box method". *Engineering science and technology an international journal*, vol. 19, pp. 1985-1992, 2016.

[31] M. E. Ali and N. Sandeep, "Cattaneo-Christov model for radiative heat transfer of magnetohydrodynamic Casson-ferrofluid: A numerical study", *Results in physics*, vol. 7, pp. 21-30, 2017.

[32] M. Mustafa,"Cattaneo-Christov heat flux model for rotating flow and heat transfer of upper-convicted Maxwell fluid", *AIP Advances*, vol. 5, no. 4, Art. ID. 047109, 2015.

[33] T. Hayat, M. I. Khan, M. Farooq, A. Alsaedi, M. Waqas, and T. Yasmeen, "Impact of Cattaneo—Christov heat flux model in flow of variable thermal conductivity fluid over a variable thicked surface", *International journal of heat and mass transfer*, vol. 99, pp. 702-710, 2016.

[34] E. Arthur, I. Seini, and L. Bortteir, "Analysis of Casson fluid flow over a vertical porous surface with chemical reaction in the presence of magnetic field", *Journal of applied mathematics and physics*, vol. 3, 713-723, 2015.

[35] M. T. Akolade, A. S. Idowu, and A. T. Adeosun, "Multislip and Soret-Dufour influence on nonlinear convection flow of MHD dissipative Casson fluid over a slandering stretching sheet with generalized heat flux phenomenon", *Heat transfer*, vol. 50, no. 4, pp. 3913-3933, 2021.

[36] A. S. Idowu, M. T. Akolade, J. U. Abubakar, and B. O. Falodun, "MHD free convective heat and mass transfer flow of dissipative Casson fluid with variable viscosity and thermal conductivity e ects", *Journal of Taibah University for Science*, vol.14, no. 1, pp. 851-862, 2020.

[37] K. V. Prasad, H. Vaidya, K. Vajravelu, and V. Ramanjini, "Analytical study of Cattaneo-Christov heat flux model for Williamson-Nanofluid flow over a slender elastic sheet with variable thickness", *Journal of nanofluids*, vol. 7, no. 3, pp. 583-594, 2018.

[38] M. M. Nandeppanavar and S. Shakunthala, "Impact of Cattaneo- Christov heat flux on magnetohydrodynamic flow and heat transfer of carbon nanofluid due to stretching sheet", *Journal of nanofluids*, vol. 8, no. 4, pp. 746-755, 2019.

[39] Z. Zhah, A. Dawar, I. Khan, S. Islam, D. L. S. Ching, and A. Z. Khan, "Cattaneo-Cristov model for electrical magnetic micropolar Casson ferrofluid over a stretching/shrinking sheet using e ective thermal con- ductivity model", *Case studies in thermal engineering*, vol. 13, Art. ID.100352, 2019.

[40] L. Fox and I. B. Parker, *Chebyshev polynomials in numerical analysis*. Oxford: Clarendon, 1968.

[41] A. S. Idowu, M. T. Akolade, T. L. Oyekunle, and J. U. Abubakar, "Nonlinear convection flow of dissipative Casson nanofluid through an inclined annular microchannel with a porous medium", *Heat transfer*, vol. 50, no. 4, pp. 3388-3406, 2021.

[42] T. L. Oyekunle, M. T. Akolade, and S. A. Agunbiade, "Thermal-di usion and di usion-thermo e ects on heat and mass transfer in chemically reacting MHD Casson nanofluid with viscous dissipation", *Applications and applied mathematics: an international journal*, vol. 16, no. 1, pp. 705-723, 2021.

[43] C. Canuto, A. Quarteroni, M. Y. Hussaini, and T. A. Zang, *Spectral methods in fluid dynamics*. Berlin: Springer, 1988.

[44] A. H. Khater, R. D. Temsah, and M. M. Hassan, "A Chebyshev spectral collocation method for solving Burgers-type equations", *Journal of computational and applied mathematics*, vol. 222, pp. 333-350, 2008.

[45] U. Ehrenstein and R. Peyret, "A Chebyshev spectral collocation method for the Navier-Stokes equations with application to double-di usive convection", *International journal for numerical methods in fluids*, vol. 9, pp. 427-452, 1989.

[46] E. M. E. Elbarbary, "Chebyshev finite di erence method for the solution of boundary-layer equations", *Applied mathematics and computation*, vol. 160, pp. 487-498, 2005.

[47] M. M. Babatin, "Numerical treatment for the flow of Casson fluid and heat transfer model over an unsteady stretching surface in the presence of internal heat generation/absorption and thermal radiation", *Applications and applied mathematics: an international journal*, vol. 13, no. 2, pp. 854-862, 2018.

[48] M. T. Akolade, "Thermophysical impact on the squeezing motion of non-Newtonian fluid with quadratic convection, velocity slip, and convective surface conditions between parallel disks", *Partial differential equations in applied mathematics*, vol. 4, Art. ID. 100056, 2021.

[49] M. T. Akolade, A. T. Adeosun, and J. O. Olabode, “Influence of thermophysical features on MHD squeezed flow of dissipative Casson fluid with chemical and radiative e ects”, *Journal of applied and computational mechanics*, vol. 7, no. 4, pp. 1999-2009, 2021.

[50] M. T. Akolade and Y. O. Tijani, “A comparative study of three dimensional flow of Casson-Williamson nanofluids past a riga plate: Spectral quasi-linearization approach”, *Partial differential equations in applied mathematics, vol. 4, Art. ID. 100108, 2021.*

[51] T. L. Oyekunle, M. T. Akolade, J. U. Abubakar, and O. T. Olotu, “Influence of variable properties on quadratic convective flow of Casson nanofluid past an inclined plane”, *Journal of applied sciences, information and computing*, vol. 2, no.1, pp. 56-67, 2021.

[52] S. Kayvan, H. Hadi, and. T. Seyed-Mohammad, “Stagnation-point flow of upper-convected Maxwell fluids”, *International journal of non-linear mechanics*, vol. 41, pp. 1242-1247, 2006.

[53] B. A. Finlayson, *The method of weighted residuals and variational principles*. New Tork, NY: Academic Press, 1972.

[54] S. Nadeema, R. U. Haqa, and C. Lee, "MHD flow of a Casson fluid over an exponentially shrinking sheet”, *Scientia iranica*, vol. 19, no. 6, pp. 1550-1553, 2012.

[55] S. Pramanik, “Casson fluid flow and heat transfer past an exponentially porous stretching surface in presence of thermal radiation”, *Ain shams engineering journal*, vol. 5, no. 1, pp. 205-212, 2014.

M. T. Akolade
Department of Mathematics,
University of Ilorin,
Ilorin,
Nigeria
e-mail: 17-68ev006pg@students.unilorin.edu.ng

A. S. Idowu
Department of Mathematics,
University of Ilorin,
Ilorin,
Nigeria
e-mail: asidowu@gmail.com
Corresponding author

B. O. Falodun
Department of Mathematics,
University of Ilorin,
Ilorin,
Nigeria
e-mail: falodunbidemi2014@gmail.com

and

J. U. Abubakar
Department of Mathematics,
University of Ilorin,
Ilorin,
Nigeria
e-mail: abubakar.ju@unilorin.edu.ng